

# A NEAR-UV SPECTROGRAPH TO INVESTIGATE THE SOLAR ATMOSPHERE.

## A SECOND GENERATION INSTRUMENT FOR DKIST.

S. Criscuoli<sup>1</sup>, F. Woeger<sup>1</sup>, T. Anan<sup>1</sup>, G. Cauzzi<sup>1</sup>, A. F. Kowalski<sup>1,2</sup>, H. Lin<sup>3</sup>

<sup>1</sup>National Solar Observatory, 3665 Discovery Drive, Boulder, CO, USA - [scriscuo@nso.edu](mailto:scriscuo@nso.edu); <sup>2</sup> University of Colorado, Boulder; <sup>3</sup> UH Institute for Astronomy.

### Synopsis

Models and preliminary studies indicate that the 300-400 nm spectral region hosts a wealth of diagnostics, fundamental for a large variety of solar studies, including abundance estimates, physics of flares, dynamo processes, atmosphere modeling and solar/stellar variability. However, due to the lower solar emission on one hand, and observational constraints on the other (seeing, scattered light and reduced optical and atmospheric transmittance), this spectral region is for the vast majority unexplored with modern instrumentation.

The diagnostic capabilities of the near-ultraviolet will be demonstrated by data that will be soon acquired by the *Sunrise* UV Spectro-Polarimeter and Imager aboard the SUNRISE III balloon-borne telescope. However, SUNRISE III will operate in a short (~days) temporal window. On the contrary, many characteristics of DKIST, including its large aperture, i.e. its high photon collecting power, even further enhanced by its ability to accommodate instruments at its Nasmyth focus, and the exceptional sky quality of the observatory site, which is characterized by low level of scattered light, make it now possible to *routinely* perform ground-based observations in the near-ultraviolet region.

*With this White Paper we make the case for a DKIST second-generation spectro-polarimeter that operates in the 300-400 nm spectral range, and lay out its high level scientific requirements.*

## Introduction

The National Science Foundation's Daniel K. Inouye Telescope is the largest optical solar telescope in the world. Its 4-m aperture allows us to observe the solar atmosphere at unprecedented spatial resolution, and with high photometric and spectropolarimetric sensitivity. The DKIST coatings and optics were designed to operate in a very broad spectral range, from 300 nm to 28  $\mu\text{m}$  (DKIST Science Requirements Document, 2005), which is also a unique capability for a high-spatial resolution facility. The five DKIST first generation instruments sample portions of this range. In particular, the shortest wavelength observable with current instrumentation is approximately 380 nm, which is sampled by the Visible Spectro-Polarimeter (de Wijn et al. 2022). Observations at wavelengths below 400 nm are notoriously difficult because: 1) the Sun is less bright so that longer exposures are needed; 2) effects of atmospheric distortion (i.e. seeing and refraction) are more severe; 3) the atmosphere's scattering is larger and 4) optics and atmospheric transmittance are often reduced in the near-ultraviolet (NUV). For these reasons, solar ground-based observations at wavelengths shorter than 400 nm, although routinely performed until the 1980s, are nowadays quite rare, and the diagnostic capabilities at these ranges are so far mostly unexplored at the temporal and spatial resolutions needed to address modern scientific questions. On the other hand, as detailed below, models and preliminary studies indicate that the NUV hosts a wealth of diagnostics fundamental for a large variety of studies, including abundance estimates, physics of flares, dynamo processes, atmosphere modeling and solar/stellar variability. These diagnostic capabilities will be soon explored by the SUSI (Feller et al. 2020) spectrograph aboard the SUNRISE III balloon, slated for launch in the next couple of years. However, SUNRISE III will operate only for a short ( $\sim$ days) temporal window. The large aperture of the DKIST, i.e. its high photon collecting power, even further enhanced by its ability to accommodate instruments at its Nasmyth focus, and the exceptional sky quality of the observatory site, which is characterized by low level of scattered light (Lin and Penn 2004), will instead make it possible to *routinely* observe in this spectral range.

*With this White Paper we make the case for a DKIST second-generation spectro-polarimeter that operates in the 300-400 nm spectral range, and lay out its high level scientific requirements.*

## Science Use Cases

**Modeling Solar and Stellar spectra.** Stellar spectra allow us to estimate the physical and chemical properties of stellar atmospheres and interiors (Molaro & Monai 2012), moreover stellar spectra and their variations affect the atmospheres of the planets they host and determine their habitability (Linsky 2019). In the case of the Sun, several measurements of its spectrum exist, but they present discrepancies whose amplitude increases at the shorter wavelengths, ranging from a few ( $\lambda > 400$  nm) to several ( $\lambda < 400$  nm) tens of percent (e.g., Doerr et al. 2016, Coddington et al. 2021). Similarly, discrepancies between synthetic spectra increase at wavelengths shorter than 400 nm (Fig.1). From the modeling perspective, uncertainties in the

computation of stellar spectra are due to various factors, which include incomplete knowledge of atomic and molecular parameters and of radiative transfer processes, and approximations employed in the calculations (e.g. Allende Prieto et al. 2003). Approximations in particular are necessary for non-LTE (non-local thermodynamic equilibrium) calculations, which are computationally very demanding, especially in 3D magnetohydrodynamic (MHD) simulations of stellar atmospheres (Nordlander et al. 2017). Such approximations and models are typically tested using the average quiet Sun as reference and consequently, their effects on spectra of atmospheres representing magnetically active areas are for the vast majority unknown. Criscuoli 2019 for instance estimated that non-LTE synthesis of NUV spectra of faculae and network performed making use of the opacity fudging approximation (e.g. Short & Hauschildt 2009) could be overestimated by tens of percent (Fig. 2). Haberreiter et al. 2021 recently showed that even continua computed with different radiative transfer codes may differ by several tens of percent across the computational domain of 3D MHD simulations.

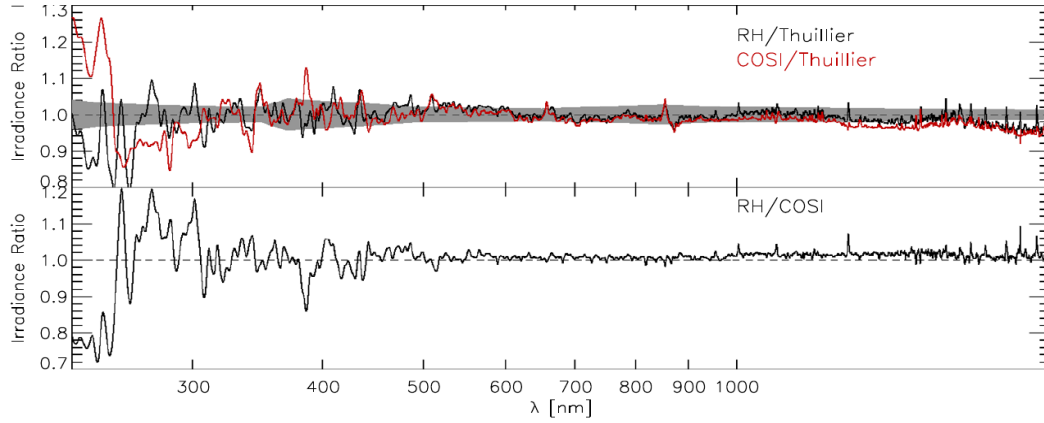


Fig. 1 Top: ratio of synthetic spectra obtained using the quiet Sun model FAL99-C with the COSI and RH radiative transfer codes, respectively, and the measured reference solar spectrum by Thuillier et al. (2004). Bottom: ratio of spectra obtained using the COSI and RH codes. The gray area represents observational uncertainties. From Criscuoli et al. 2020.

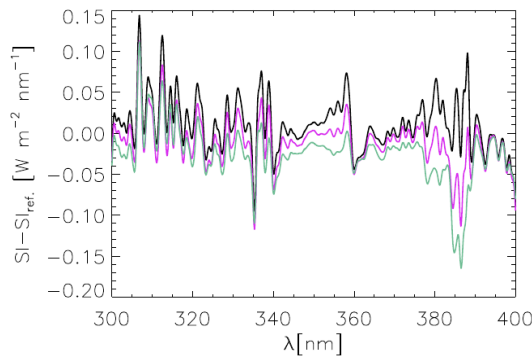


Fig. 2: Difference between Spectral Irradiance computed using a complete molecular line list in the UV ( $SI_{ref}$ ) and a synthesis performed instead fudging the UV opacity ( $SI$ ). Different colors represent different model atmospheres. Black: center cell. Pink: network. Green: plage. From Criscuoli 2019.

Spatially resolved ( $\leq 0.1$  arcsec to resolve magnetic magnetic bright-points) NUV spectra of surface features characterized by different levels of activity will allow for the first time to validate radiative transfer approaches and approximations in regions different from the quiet Sun. A broad spectral region of 1 to 50 nm should be observed, with a resolution of  $R \sim 10^4 - 10^5$ , in order

to properly sample a sufficient number of atomic and molecular lines relevant for the computation of UV opacities.

**Multi-line spectroscopy and spectro-polarimetry in the UV range.** Investigations of the solar atmosphere have long relied on the use of observations in a few specific spectral regions. For instance, classic spectrographs, and bi-dimensional spectrographs attached to telescopes such as SST, GREGOR, DST, GST, and HINODE observe in limited subsets of a few Fe I lines (e.g. 630.1/630.2, 617.3, 525.0 nm, 1.5  $\mu$ m), He I 1083.0 nm, Na D I, H $\alpha$ , Ca II H&K and IR. On the other hand, several works have recently demonstrated the superiority of using multi-line spectroscopy and spectropolarimetry in retrieving the physical and magnetic properties of solar plasma. For instance Quintero Noda et al. 2017, 2019 compared inversions performed with the Ca II 854.2 nm with inversions performed using several lines in the 850 nm range, and found that the latter better retrieves both photospheric and chromospheric parameters. Kuckein et al. 2021 showed that the simultaneous inversion of Stokes I of 15 lines in the Cr I 578.1 nm range allows to reliably retrieve both plasma and magnetic fields properties. The first generation ViSP instrument attached to the DKIST can observe combinations of three, 1 nm spectral windows within the range 380 and 900 nm, thus allowing multi-line spectroscopy/ spectropolarimetry. Indeed, Ruiz Cobo et al. 2022 recently showed that 13 lines in the Fe I 630.1/630.2 nm and Ca II IR spectral ranges, compatible with ViSP observational setups, can be successfully inverted with the DeSIRE code to reliably provide estimates of the properties of the solar photosphere and chromosphere. Riethmüller and Solanki 2019 pushed this concept further, comparing results obtained inverting hundreds of lines at the same time, and showed that the 300-430 nm range is particularly suitable due to the high density of lines, which allow to better constrain (by a factor of three or better) the parameters of the upper-atmosphere than inversions performed in the Visible (around the 630.2 nm line). Multiline spectropolarimetry was indeed one of the main goals that drove the development of the instrument SUSI, aboard the SUNRISE III balloon-borne telescope.

The proposed instrument will *routinely* acquire spectro-polarimetric observations in wide ( $\sim 2$  nm) spectral regions at high spectral ( $R \sim 10^5$ ) and spatial resolution ( $\leq 0.1$  arcsec to resolve magnetic and convective fine structures). Combining its observations with data acquired with other DKIST instruments at longer wavelengths *will allow a better derivation of the properties of the solar plasma and magnetic fields at different heights in the atmosphere, from the photosphere to the chromosphere*. This capability, in turn, will allow addressing several science questions, which include validating and improving solar atmosphere models, investigating the fine structuring of the solar magnetic fields and their dynamics, understanding reconnection events, and so on.

**Understanding solar-stellar variability and Proxy magnetometry.** The 320-400 nm region is rich with molecular lines, such as OH, NH, CH and CN. CN observations in particular are employed for proxy magnetometry, as the contrast of magnetic features appears particularly

bright in filters centered at the CN bandhead (Uitenbroek & Tritschler 2007). This brightness increase modulates disk-integrated solar radiation measurements over the solar rotation (Marchenko et al. 2021) and the 11-years cycle, so that measurements in the CN band can be employed as proxy of solar and stellar magnetic activity (e.g. Livingston 2007).

The model by Shapiro et al. 2015 showed that other molecules in this range produce appreciable variability over the cycle, and that on the solar-rotation temporal scale the variability of these lines is larger than the one of molecular lines located at longer wavelengths (e.g. G-band). *High-spectral resolution ( $R \sim 10^5$ ) spectro-polarimetric observations acquired in the NUV with the proposed instrument will allow us to investigate the detailed physical processes determining such variations, characterize the magnetic field-brightness relation and explore the use of new magnetic activity proxies.*

**White-Light Flares.** Flares are the result of dynamic magnetic field reconfiguration above the stellar surface, which dramatically heats the surrounding atmosphere. During both solar and stellar flares, emission is seen as line and continuum radiation from X-ray to radio wavelengths, with the majority of the radiative energy release occurring in the optical and NUV continuum (Woods et al. 2004). This is commonly referred to as the white-light continuum. Solar imaging data shows convincingly that this emission is spatially and temporally coincident with the impulsive heating by nonthermal electrons inferred from hard X-rays (Neidig & Kane 1993, Fletcher et al. 2007), with recent interpretations invoking radiative backwarming to explain the white-light emitted at low layers (e.g., Isobe et al. 2007). However, direct measurements of unprecedented low source regions of optical flare sources on the limb are now challenging this typical paradigm of nonthermal electron energy transport from the corona to the chromosphere and radiative backheating of the photosphere (Martinez-Oliveros et al. 2012).

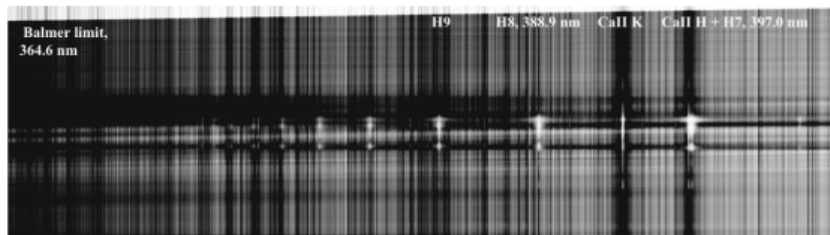


Fig. 3 Slit spectra of the white light flare analyzed in Neidig (1983). The y-axis corresponds to the spatial direction on the Sun, while the x-axis is the wavelength dispersion, between the Balmer limit and  $\sim 400$  nm. In the flaring kernel both the CaII H&K resonance lines, and the high order H Balmer lines are clearly seen in emission.

Spectral coverage at  $< 400$  nm would represent a unique opportunity to investigate flaring emission in the lower solar atmosphere. As clearly seen in the 1983 spectra of Fig. 3, the Ca II H & K lines exhibit narrow profiles (which can be used to constrain the turbulence) in comparison to the hydrogen Balmer series, which broaden and merge due to the Stark effect. An example of the series merging is shown in Fig. 4 (left panel). By observing these optically thin Balmer lines

at NUV wavelengths (365-376 nm), the electron density attained through deep heating of the chromosphere can be determined (whereas optically thick lines like H $\alpha$  are formed much higher up in the flare atmosphere), thus allowing to estimate the high energy part of the non-thermal particle's energy spectra. Recently, self-consistent calculations of the broadening of these lines has become possible in flare models (Kowalski et al. 2022).

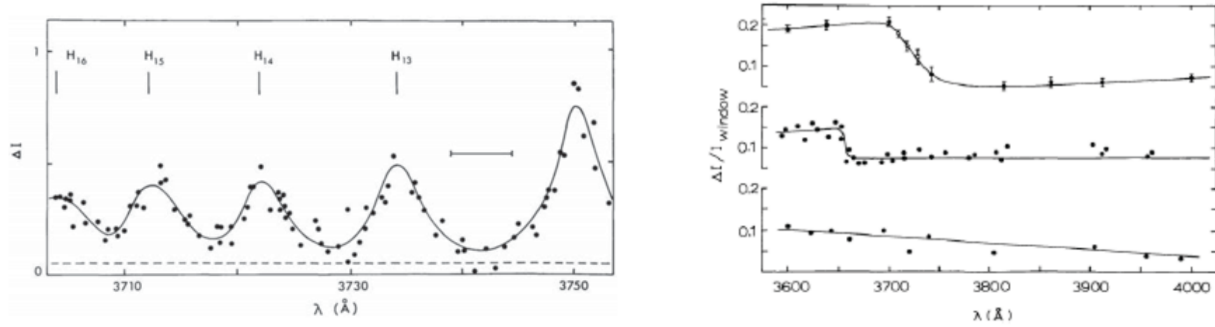


Fig. 4 - Left: Spectrum of the merging of the high-order (H12-H16) Balmer series during a flare (from Neidig 1983). Right: Compilation of Balmer jump spectra of several solar flares from Hiei 1982, Neidig 1983, and Machado 1974; note that due to uncertainty in pointing in these older data, it is not known exactly whether these spectra were acquired in the brightest flaring kernels.

However, these important diagnostics have not been comprehensively observed with any spatial resolution since the early 1980s. Another example is shown in Fig. 4 (right), as a composite of several continuum spectra covering the Balmer limit (364.6 nm): the wide range of shapes has not been explained or systematically investigated with newer observations. Indeed, the only modern constraints on the solar flare continuum distribution are provided by composites of narrowband imaging data from instruments with largely disparate spatial resolutions (e.g., Kerr et al. 2014, Kleint et al. 2016).

*The proposed spectrograph will allow observation of a spectral region ( $\sim 50$  nm) wide enough to characterize the strength and location of the Balmer continuum jump, and with a spectral resolution ( $R \sim 10^4$ ) suitable to resolve variations of higher-order Balmer lines.*

**A wealth of new diagnostics: abundances, continuum polarization and Hanle effect, coronal physics.** The 300-400 nm spectral range offers a wealth of additional diagnostics, still unexplored for the large part. Amarsi et al. 2021 showed how lines of OH, NH, CH and CN can be employed to estimate the highly debated abundance of C, N and O in the solar atmosphere. Berdyugina et al. 2002, 2003 showed that molecular lines in this range, especially OH, are good diagnostics of sunspot and stellar magnetic fields. Weak (1-10 G), turbulent magnetic fields in the quiet Sun can also be investigated, via the Hanle effect. Molecular lines in particular are well suited for the Hanle differential diagnostic technique, due to the fact that while they form essentially in the same atmospheric conditions, different branches may have different sensitivity to the magnetic field: their ratio removes the dependence on atmospheric models' assumptions,

thus allowing a better estimation of the magnetic field (e.g. Kleint et al. 2010). Scattering (linear) polarization is particularly strong in the near UV, and very sensitive to details of atmospheric stratification. Trujillo Bueno and Schukina 2009 therefore suggested using continuum linear polarization center-to-limb observations in this range, to validate solar atmosphere models. Finally, exploratory studies of the solar corona would be extremely interesting: a number of strong coronal lines is expected in this spectral range (Del Zanna & De Luca 2018), including lines from several charge states of Fe (from Fe IX to Fe XIII), that can be used to directly address the charge states of the nascent solar wind. The coronagraphic quality of the Haleakala sky, as well as the DKIST design make this a unique opportunity. Note that the last two science cases would require a sensibly lower spectral and spatial resolution, in order to achieve enough polarimetric sensitivity, or properly measure the relatively low coronal emission.

### **High-level definition of a spectro-polarimeter in the ultraviolet wavelength regime for DKIST**

Rooted in the scientific questions raised above, we propose a spectro-polarimeter that operates at ultraviolet wavelengths below 400 nm, limited only by the transmission absorption by Earth's atmosphere that becomes severe below 320 nm. The high-level requirements for an instrument adequate to acquire the necessary data products are summarized in the table below.

<b>Item</b>	<b>Requirement</b>
Wavelength Range	320-400 nm
Spatial Resolution	$\leq 0.1$ arcsec
Spectral resolving power	15000 (low resolution mode) 100000 (high resolution mode)
Spectral bandwidth	50 nm (low resolution mode) 2 nm (high resolution mode)
Polarimetric data acquisition	Dual beam polarimeter
Polarimetric Sensitivity	$10^{-4} S / I_{\text{cont}}$ , for all Stokes parameters S
Field of View	2x2 arcmin square, or larger
Temporal resolution	<30s to achieve $10^{-4} S / I_{\text{cont}}$ required spatial and spectral resolution, and for all Stokes parameters S <10s in spectral mode for flare studies.
Simultaneously observed wavelength bands	1

Scan accuracy	0.05 arcsec equivalent on-sky positioning
Multi-instrument observations	Possible with other DKIST instrumentation

An image slicer would be the ideal for flare studies, although studies requiring high spectropolarimetric sensitivity would benefit as well (del Pino Aleman et al. 2021).

## **Integration with DKIST**

The Nasmyth station - integrated part of DKIST's design to allow for future instrumentation upgrades - provides an excellent location option for the proposed instrument, in particular due to its high throughput at wavelengths below 400 nm (DKIST Science Requirements Document, 2005). For co-observations with other DKIST instrumentation, the light feed to the DKIST coude floor that hosts the instruments for observations in the visible and infrared wavelength regime requires expansion. We propose a dichroic beam splitter as the optical element to direct the wavelength band below 400 nm to the Nasmyth focus. Optics with such coatings are possible for large substrates (Harrington et al. 2021). There are generally no major technical challenges with the proposed instrument, although an adaptive optics system may need to be integrated with the instrument to achieve the required spatial resolution. An instrument of this character is not unsimilar to the Visible Spectro-Polarimeter or the Diffraction Limited Near Infrared Spectropolarimeter in complexity, and would carry the typical cost for a DKIST instrument of the order of ten million dollars and a multi-year design and fabrication phase duration. More exact numbers will have to be established based on final scope at the end of a preliminary design phase.

## **Summary**

In this White Paper we make the case for a DKIST second-generation spectro-polarimeter that operates in the 300-400 nm spectral range, a region of the spectrum that has been so far mostly unexplored with spatially resolved observations. We show that several science cases can be addressed by a spectrograph that operates at different spectral resolutions thus allowing observations in both broad ( $\sim 50$  nm) and narrow ( $\sim 2$  nm) spectral windows. Combining data from the proposed instrument with data acquired with other DKIST instrumentation, will additionally allow to simultaneously collect spatially resolved observations in unprecedentedly wide spectral regions, from the NUV to the Infrared. The proposed instrument addresses the following Decadal Survey for Heliophysics 2024-2033 statement of task: i. The structure of the Sun and the properties of its outer layers in their static and active states; ii. The characteristics and physics of the interplanetary medium from the surface of the Sun to interstellar space beyond the boundary of the heliosphere.



## References

- Allende Prieto, C., Hubeny, I., & Lambert, D. L. 2003, ApJ, 591, 1192. [10.1086/375527](#)
- Amarsi, A. M., Grevesse, N., et al. 2021, A&A, 656, A113. [10.1051/0004-6361/202141384](#)
- Berdyugina, S. 2002, AN, 323, 192. [10.1002/1521-3994\(200208\)323:3/4<192::AID-ASNA192>3.0.CO;2-U](#)
- Berdyugina, S. V., Solanki, S. K., & Frutiger, C. 2003, A&A, 412, 513. [10.1051/0004-6361:20031473](#)
- Criscuoli, S. 2019, ApJ, 872, 52. [10.3847/1538-4357/aaf6b7](#)
- Criscuoli, S., Rempel, M., Haberreiter, M., et al. 2020, SoPh, 295, 50. [10.1007/s11207-020-01614-2](#)
- Coddington, O.M., Richard, E.C., Harber, D., et al. Geophys. Res. Lett. 2021, 48, e2020GL091709. [10.1029/2020GL091709](#)
- de Wijn A. G., Casini R., Carlile A., et al., 2022, SoPh, 297, 22. [doi:10.1007/s11207-022-01954-1](#)
- del Pino Aleman, T., Trujillo Bueno, J. 2021, ApJ, 901, id.80. [10.3847/1538-4357/abdd25](#)
- Del Zanna, G. & De Luca, E. E., 2018, ApJ 852, 52. [https://doi.org/10.3847/1538-4357/aa9edf](#)
- Doerr, H.-P., Vitas, N., & Fabbian, D. 2016, A&A, 590, A118. [10.1051/0004-6361/201628570](#)
- DKIST Science Requirements Document, Revision B, 2005, [https://dkist.nso.edu/sites/atst.nso.edu/files/docs/SPEC-0001-B.pdf](#)
- Fletcher, L., Hannah, I. G., Hudson, H. S., & Metcalf, T. R. 2007, ApJ, 656, 1187. [10.1086/510446](#)
- Haberreiter, M., Criscuoli, S., Rempel, M., & Pereira, T. M. D. 2021, A&A, 653, A161. [10.1051/0004-6361/202039237](#)
- Harrington D. M., Wöger F., et al., 2021, JATIS, 7, 048005. [doi:10.1117/1.JATIS.7.4.048005](#)
- Isobe, H., Kubo, M., Minoshima, T., et al. 2007, PASJ, 59, S807. [10.1093/pasj/59.sp3.S807](#)
- Kowalski, A. F., Allred, J. C., Carlsson, M., et al. 2022, ApJ, 928, 190. [10.3847/1538-4357/ac5174](#)
- Kerr, G. S., & Fletcher, L. 2014, ApJ, 783, 98. [10.1088/0004-637X/783/2/98](#)
- Kleint, L., Berdyugina, S. V., Shapiro, A. I., & Bianda, M. 2010, A&A, 524, A37. [10.1051/0004-6361/201015285](#)
- Kleint, L., Heinzel, P., Judge, P., & Krucker, S. 2016, ApJ, 816, 88. [10.3847/0004-637X/816/2/88](#)
- Kuckein, C., Balthasar, H., Quintero Noda, C., et al. 2021, A&A, 653, A165. [10.1051/0004-6361/202140596](#)
- Lin, H., Penn, M.J.: 2004, *Publ. Astron. Soc. Pac.* **116**, 652. [10.1086/422205](#)
- Linsky, J. 2019, Host Stars and Their Effects on Exoplanet Atmospheres, Vol. 955 (Berlin: Springer). [10.1007/978-3-030-11452-7](#)
- Livingston, W., Wallace, L., White, O. R., Giampapa, M. S. 2007, ApJ, 657.1137L. [10.1086/511127](#)
- Marchenko, S., Criscuoli, S., DeLand, M. T., Choudhary, D. P., & Kopp, G. 2021, A&A, 646, A81. [10.1051/0004-6361/202037767](#)
- Martínez Oliveros, J.-C., Hudson, H. S., et al. 2012, ApJL, 753, L26. [10.1088/2041-8205/753/2/L26](#)
- Molaro, P., & Monai, S. 2012, A&A, 544, A125. [10.1051/0004-6361/201118675](#)
- Neidig, D. F. 1983, SoPh, 85, 285. [10.1007/BF00148655](#)
- Neidig, D. F., & Kane, S. R. 1993, SoPh, 143, 201. [10.1007/BF00619106](#)
- Nordlander, T., Amarsi, A. M., Lind, K., et al. 2017, A&A, 597, A6. [10.1051/0004-6361/201629202](#)
- Quintero Noda, C., Iijima, H., Katsukawa, Y., et al. 2019, MNRAS, 486, 4203. [10.1093/mnras/stz1124](#)
- Quintero Noda, C., Shimizu, T., Katsukawa, Y., et al. 2017, MNRAS, 464, 4534 [10.1093/mnras/stw2738](#)
- Riethmüller, T. L., & Solanki, S. K. 2019, A&A, 622, A36. [10.1051/0004-6361/201833379](#)
- Ruiz Cobo, B., Quintero Noda, C., et al. 2022, A&A, 660, A37. [10.1051/0004-6361/202140877](#)
- Shapiro, A. I., Solanki, S. K., Krivova, N. A et al. 2015, A&A, 581, A116. [10.1051/0004-6361/201526483](#)
- Short, C. I., & Hauschildt, P. H. 2009, ApJ, 691, 1634. [10.1088/0004-637X/691/2/1634](#)
- Trujillo Bueno, J., & Shchukina, N. 2009, ApJ, 694, 1364. [10.1088/0004-637X/694/2/1364](#)
- Uitenbroek, H., & Tritschler, A. 2007, A&A, 462, 1157. [10.1051/0004-6361:20066286](#)
- Woods, T. N., Eparvier, F. G., Fontenla, J., et al. 2004, GeoRL, 31, L10802. [10.1029/2004GL019571](#)